



IRWIN AND JOAN JACOBS
CENTER FOR COMMUNICATION AND INFORMATION TECHNOLOGIES

Generalized Laplacians and Curvatures for Image Analysis and Processing

**Eli Appleboim, Emil Saucan,
Gershon Wolansky and
Yehoshua Y. Zeevi**

CCIT Report # 774
August 2010

 Electronics
Computers
Communications

DEPARTMENT OF ELECTRICAL ENGINEERING
TECHNION - ISRAEL INSTITUTE OF TECHNOLOGY, HAIFA 32000, ISRAEL



Generalized Laplacians and Curvatures for Image Analysis and Processing

Eli Appleboim¹ Emil Saucan² Gershon Wolansky² and Yehoshua Y. Zeevi¹

1- EE. Dept. 2- Math. Dept.
Technion Haifa Israel

Abstract. Newly developed combinatorial Laplacians and curvature operators for grayscale, as well as color images are tested on 2D synthetic and natural images. This novel approach is based upon more general concepts developed by R. Forman and is inspired by the Bochner-Weitzböck formula which is an essential identity in Riemannian Geometry. After the presentation of the operators as they operate on images we further demonstrate the implementation of them as diffusion kernels. The differences between the various Laplacians we define, are illustrated by these examples as each of the operators is shown to be adequate for different type of image processing tasks such as sharpening anomaly detection smoothing and denoising.

1 Introduction and Related Works

Diffusion methods, and in particular those based upon the Laplacian in general, and the heat equation in particular, belong by now to the basic repertoire of methods available to the (geometric) Image Processing community (see, e.g. [25], [1], [13], [23], [24], [27] and references therein). As such, the relevant literature is by far too extensive for us to attempt here even an incipient bibliography.

Also, curvature analysis is of great importance in Image Processing, Computer Graphics, Computer Vision and related fields, for example in applications such as reconstruction, segmentation and recognition (e.g. [6], [14], [22], [28], [13], [1]). The conventional approach embraced in most studies implements curvature estimation of a polygonal (or, more generally, polyhedral) mesh or a grid, approximating the supposedly smooth (C^2) image under study. The curvature measures of the mesh converge in this case to the classical, differential, curvature measure of the investigated surface.

Stimulated by Perelman's seminal work on the Ricci flow [18], [19], and by its application in the proof of Thurston's Geometrization Conjecture, and, implicitly of the Poincaré Conjecture ([17]), resulting in discrete versions of the Ricci flow and related flows ([5], [10], [15]), Ricci curvature (and Ricci flow) penetrated the main stream of Imaging and Graphics, starting with the works of Gu et al (see, e.g. [29]).

Ricci curvature measures the deviation of the manifold from being locally Euclidean in various tangential directions. More precisely, it appears in the second term of the formula for the $(n - 1)$ -volume $\Omega(\varepsilon)$ generated within a solid angle (i.e. it controls the growth of measured angles).

$$\mathbf{v} \cdot \text{Ricci}(\mathbf{v}) = \frac{n-1}{\text{vol}(\mathbf{S}^{n-2})} \int_{\mathbf{w} \in T_p(M^n), \mathbf{w} \perp \mathbf{v}} K(\langle \mathbf{v}, \mathbf{w} \rangle), \quad (1)$$

where $\langle \mathbf{v}, \mathbf{w} \rangle$ denote the plane spanned by \mathbf{v} and \mathbf{w} , and $K(\langle \mathbf{v}, \mathbf{w} \rangle)$ is the sectional curvature relative to that plane via the exponential map. i.e. Ricci curvature represents an average of sectional curvatures. The analogy with mean curvature is further emphasized by the fact that Ricci curvature behaves as the Laplacian of the metric g ([4]).

We should note that while sectional curvature measures *geodesic deviation*, i.e. the relative separation of geodesics close to a reference geodesic (see, e.g. [4], [4]), Ricci curvature measures the average geodesic deviation over all planes containing a given initial direction (as can be inferred from the mentioned property of sectional curvature and from Equation (1.1)). It is precisely this property that it is used in [7], [3] to analyze the stability, coherence of brain fibers using DTI (Diffusion Tensor Imaging).

It is also important to note that in dimension $n = 2$, which is the most relevant to classical Image Processing and its related fields, Ricci curvature reduces to the classical Gauss curvature.

Bochner-Weitzenböck Identity Given a function f defined in some \mathbb{R}^n its Laplacian is (up to sign) the well known differential operator

$$\Delta f = \text{div} \nabla f = \text{tr}(\text{Hess} f) = \sum \frac{\partial^2}{(\partial x_i)^2} f$$

Yet, on Riemannian manifold the situation is different and there are several self adjoint operators named Laplacian. In general, each of which acts on differential forms ([4], [20], [4]).

Differential forms represent an important theoretical tool of differential geometry and modern analysis. Roughly speaking these are generalization of the notion of differential of function defined on \mathbb{R}^n , to functions defined on Riemannian manifolds. In this terminology functions are 0-order differential forms. Recently they found their way in imaging and graphics, starting with the work of Gu and Yau [11].

A property that relates Laplacians on a manifold with its geometry (through curvature) – and the one that stands at the heart of this paper – is the classical *Bochner-Weitzenböck* formula, that for functions, has the form (see, e.g. [4], [20]),

$$-\frac{1}{2} \Delta (\|df\|^2) = \|\text{Hess} f\|^2 - \langle df, \Delta df \rangle + \text{Ric}(df, df). \quad (2)$$

Here $\text{Hess} f$ denotes the Hessian of a function f : $\text{Hess} f = \nabla df = \nabla^2 f$ and $\langle \cdot, \cdot \rangle$ as usual, the inner product, and Δ is the Laplacian operator.

For a proof, the reader can consult, e.g. [20], but he can find a shorter and somewhat less technical proof along the same lines in [12]. Both variants of the proof emphasize Ricci curvature as appearing in the formula for the Jacobian

determinant of the exponential map. However, a different proof, based upon Eulerian approach to mechanics arguments can also be found in [26].

Extended to differential forms, the Bochner-Weitzenböck identity relates the *rough* laplacin \square and the *Bochner* Laplacian, and, in its most compressed version states that,

$$\square_p = dd^* + d^*d = \nabla_p^* \nabla_p + \text{Curv}(R), \quad (3)$$

We adopt the notation \square for the rough Laplacian (also known as Hodg de-Rahm Laplacian) from [8] which we will follow more closely in the next section. It is defined as the trace of the Hessian (se [4], [20]) of the p -form ω :

$$\square\omega = -\text{tr}_g \nabla^2 \omega,$$

Acting on functions (0-differential forms) it coincides with the Laplace-Beltrami operator. $\nabla_p^* \nabla_p$ is the *Bochner Laplacian* and $\text{Curv}(R)$ is a quite complicated expression with linear coefficients of the *curvature tensor* R ([4], [20]). (Here ∇_p is the *covariant derivative* operator.)

In the work of Forman [8], combinatorial analogues of the rough Laplacian, bochner Laplacians and curvature are defined. These operators are introduced in [8] in the context of cell-complexes. We will not elaborate herein on the basics of cell-complexes and their essential role in topology and geometry and just state that, roughly speaking, one can think of a grid, mesh or triangulation as examples of cell complexes. Every Riemannian manifolds possesses a cell complex structure ([16]).

The paper is organized as follows. In Section 2 we will describe our proposed adaptation of the combinatorial operators defined by Forman to images and give some examples of their computations. In Section 3 we describe applications of these operators for diffusion processes implemented on images, and bring some experimental results. Finally, Section 4 summarizes the paper and some work in progress and future studies are discussed.

2 Applications - From Riemannain Manifolds to Images

In this section we introduce our proposed implementation of the operators coupled in the Weitzenböck identity namely, the *rough* and *Bochner* Laplacians and the *curvature* term, for images. This is based on the operators as defined in [8]. We will not describe Forman's formulation in details, but introduce only the adaptation we took for images. Before defining the operators we have to introduce the cellular decomposition we attach to images. This comes natural, as it is induced by the *grid* of an image. The 2-cells are the pixels themselves while the 1-cells are the vertical and horizontal edges formed by adjacent pixels. This is illustrated in Figure 1. In fact, one should bare in mind that since we regard images as manifolds (usually surfaces) we need the cellular decomposition to be defined on the image surface. In this context, the 2-cells are actually the surface elements of the form $I(p)$, where $p = (i, j)$ is the (i, j) pixel of the image I , and the 1-cells are the arcs $I(e)$ where e is either vertical or horizontal edge

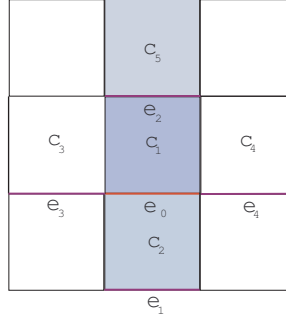


Fig. 1. Cell decomposition of an image

between adjacent pixels. Along the following expressions, all terms w represents weight functions ([8]). These functions are supposed to reflect geometric entities such as length, area, volume etc. All terms including 3-cells in the definitions of the operators are assumed to vanish since we regard images as surfaces, i.e. cell complexes of maximal dimension 2.

A word about notation: When α represents a p -dimensional cell (p -cell - in the framework of this paper $p = 1, 2$), the notation $\beta < \alpha$ (resp. $\alpha < \beta$), means that β is a $(p-1)$ -cell ($(p+1)$ -cell) which is a face of α (α is a face of β). Following [8] we define,

2.1 Combinatorial Operators

1-forms: Rough Laplacian, Ricci Curvature and Bochner Laplacian

Definition 1. 1. The combinatorial rough Laplacian of I at e_0 is defined as

$$\square_1(e_0) = \frac{w(e_0)}{w(c_1)} - \frac{w(e_0)}{w(c_2)}. \quad (4)$$

2. The Ricci curvature of I along e_0 is given as

$$\text{Ric}(e_0) = w(e_0) \left[\left(\frac{w(e_0)}{w(c_1)} + \frac{w(e_0)}{w(c_2)} \right) - \left(\frac{\sqrt{w(e_0)w(e_1)}}{w(c_1)} + \frac{\sqrt{w(e_0)w(e_2)}}{w(c_2)} \right) \right]. \quad (5)$$

3. We define the Bochner 1-Laplacian of I at e_0 , to be

$$B_1(e) = \square_1(e) - \text{Ric}(e) \quad (6)$$

2-forms: Rough Laplacian, Curvature and Bochner Laplacian

Definition 2. With the same notation as before regarding 3-dimensional as zero weighted, we define the following.

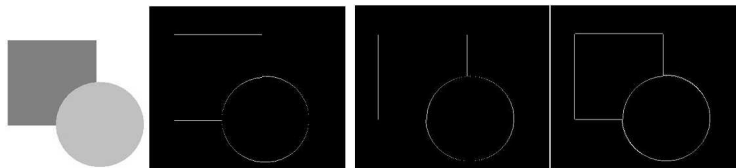


Fig. 2. Ricci curvature of a test image. Vertical, Horizontal and coupled

1. The rough Laplacian \square_2 , is given by

$$\square_2(c_1, c_2) = \frac{w(e_0)}{\sqrt{w(c_1)w(c_2)}}. \quad (7)$$

2. The 2-curvature measure \mathcal{F}_2 say, for the 2-cell (pixel) c_1 , is defined to be,

$$\mathcal{F}_2 = \sum_{e < c_1} \frac{w(e)}{w(c_1)} - \sum_{\substack{i=2 \\ e < c_1, e < c_i}}^5 \frac{w(e)}{\sqrt{w(c_1)w(c_i)}}. \quad (8)$$

Note that for pixels in the boundary of an image, some of the terms in the second summand vanish, since not all four neighboring pixels exist. However, for pixels that are not boundary pixels the expression of the curvature \mathcal{F}_2 can be simplified to,

$$\mathcal{F}_2 = \sum_{e < c_1} \left(\frac{w(e)}{w(c_1)} - \frac{w(e)}{\sqrt{w(c_1)w(c_i)}} \right). \quad (9)$$

3. The Bochner 2-Laplacian B_2 , is set to be,

$$B_2 = \square_2 - \mathcal{F}_2. \quad (10)$$

2.2 Weightening

In this subsection we address the issue of which weights should be imposed for the w 's. We will review two essential schemes for weightening, a purely combinatorial one and a geometric one. While it is unlikely to have an optimal set of weights, the geometric scheme seems to be superior over the combinatorial one in terms of quality of obtained results however, more expensive in terms of computing resources. As noted in the previous subsection, in both schemes 3-dimensional cells are zero weighted. Considering 3-cells, as well as, applying the methods presented herein for higher dimensional signals, and also to computer graphic oriented tasks, is currently in progress or left for future work.

Combinatorial Weightening In this scheme the weights are taken to be merely the gray level at a given pixel for $w(c)$ of a 2-cell, and the average of gray levels of pixels adjacent along an edge e is taken as $w(e)$. Figure 3 show examples of Ricci curvature with combinatorial weights.



Fig. 3. Ricci curvature with combinatorial weights

Geometric Weights While combinatorially weighting of cells is simple and efficient for computation, we would still like to account for the image geometry. The most natural way to do this would be to define the weights $w(e)$ and $w(c)$ in a way so they would reflect length and area respectively. The basic way to do that is through the metric of the image as it is considered as a surface embedded in \mathbb{R}^n , through the embedding $I(X, Y)$. For gray level images the embedding is into \mathbb{R}^3 while for color images \mathbb{R}^5 is taken ([23]). Using standard differential geometry [4], [4] and its adaptation to images ([23], [13], [24] and many others), the metric of a gray level image is given by the matrix

$$\mathcal{G}_{i,j} = \begin{pmatrix} 1 + I_x^2 & I_x I_y \\ I_y I_x & 1 + I_y^2 \end{pmatrix} \quad (11)$$

As a matter of fact one can take a parameterized version of the metric with a parameter β in the form of

$$\mathcal{G}_{i,j} = \begin{pmatrix} \beta + I_x^2 & I_x I_y \\ I_y I_x & \beta + I_y^2 \end{pmatrix} \quad (12)$$

The parameter β scales the differential change of the image dI with respect to the spatial differential of X and Y , dX, dY respectively thus enabling one to

be more sensitive or less sensitive to image gradient (i.e. presence of edges - see [23]).

For color images rendered as surfaces embedded in \mathbb{R}^5 with coordinate system $I = (X, Y, R(X, Y), G(X, Y), B(X, Y))$ the parameterized metric is given by

$$\mathcal{G}_{i,j} = \begin{pmatrix} \beta + R_x^2 + G_x^2 + B_x^2 & R_x R_y + G_x G_y + B_x B_y \\ R_x R_y + G_x G_y + B_x B_y & \beta + R_x^2 + G_x^2 + B_x^2 \end{pmatrix} \quad (13)$$

However, for simplicity considerations, in this work we are taking into account the stretch only in the horizontal and vertical directions which amounts to replacing the full metric tensor with the following horizontal (resp. vertical) length element of a horizontal (vertical) edge $e_x(e_y)$ (the weight of e) is defined as

$$w(e_x) = ds(e_x) = \sqrt{\beta + I_x^2} dx ; w(e_y) = ds(e_y) = \sqrt{\beta + I_y^2} dy . \quad (14)$$

The area element above a pixel can be given at a “first order approximation” by,

$$dA = ds_x ds_y . \quad (15)$$

A more comprehensive version of area element would be obtained by subdividing a pixel to triangles say, and taking the sum of areas of the triangles.

Examples Figures 4 to 6 show the results of computing \square , Ricci curvature and Bochner Laplacian with geometric weights.



Fig. 4. \square with geometric weights: From left to right, original image, \square_1 and \square_2

In Figure 7 the significance of the parameter β is illustrated. It is observed that as β is increased from 5 to 15 to 25 more edges are detected.



Fig. 5. Ricci curvature with geometric weights. Notice the explicit detection of edges. This should be expected, as at the presence of edges curvature is expected to be significantly higher than in homogenous areas



Fig. 6. B with geometric weights: Left to right - Original, B_1 and B_2

3 Uses - Diffusion Processes

In recent years diffusion processes have become state of the art in images processing playing an important role in a variety of image processing tasks. Applications range from denoising to segmentation to texture analysis and anomaly detection and many more (see [1], [13], [23], [24], [9], [27]). The basic linear diffusion of an image, $I(X,Y)$ is the operation defined by

$$\frac{\partial I}{\partial t} = \Delta I . \quad (16)$$

Where $\Delta I == tr(HessI) = I_x^2 + I_y^2$ is the Laplacian of the image regarded as a function of X and Y . When considering images as Riemannian manifolds it is common, and very useful to deal with color images to replace the Laplacian above with the Laplace-Beltarmi operator which acts on the metric of the image ([13], [24], [27], [21]). The diffusion in the Beltrami framework takes the form of

$$\frac{\partial I}{\partial t} = \Delta_g I . \quad (17)$$



Fig. 7. Ricci curvature with different values of β : From left to right β ranges from 5 to 15 to 25. As the value of β increases the scaling between the gradient of the image dI with respect to the change of image coordinates dX, dY changes and consequently sensitivity to edges. High values of β detects more edges than small values.

$\Delta_{\mathcal{G}}I$ is the Laplacian of the metric of I (Laplace-Beltrami operator) given in coordinates by, ([4], [20])

$$\Delta_{\mathcal{G}}I = \frac{1}{\sqrt{\det(\mathcal{G})}} \sum_{i,j=1}^2 \frac{\partial}{\partial X^i} (\sqrt{\det(\mathcal{G})} \mathcal{G}^{i,j} \frac{\partial I}{\partial X^j}). \quad (18)$$

We used the convention that $(X^1, X^2) = (X, Y)$ are the spatial coordinate of the image (pixels). In light of the above and equipped with the Laplacian operators described in the previous section we have followed in two directions. One was to use each of the operators defines previously as a diffusion kernel instead of the Laplace-Beltrami operator. Meaning that we have applied the following process,

$$\frac{\partial I}{\partial t} = \mathcal{O}pI \quad (19)$$

while at each time substituting $\mathcal{O}p$ with each of the operators \square_1 and \square_2 . Additionally, in the spirit of the Weitzenböck identity, we have applied Bochner Laplacian from its decomposition to \square and $Curv$, and compared the obtained results to a straight forward implementation of Beltrami flow.

3.1 Results

In all applications shown below weights where taken as geometric weights as these tend to produce better results.

\square_1 as a sharpening operator The 1-form laplacian \square_1 acts on 1-cells and as such have the tendency to flatten edges. Taken with a minus sign in a diffusion process of the form

$$\frac{\partial I}{\partial t} = -\square_1 I.$$

will in turn enhance its edges as seen in Figure 8. This results with a good candidate for image sharpening task. Figure 8 shows an image that is sharpened using the process defined above.



Fig. 8. Applying $\frac{\partial I}{\partial t} = -\square_1 I$: Top shows the original image and on the bottom its sharpened version

\square_2 **Detects anomalies** As the Laplacian \square_2 acts on two cells it can be regarded as the dual of the 1-Laplacian \square_1 . Applied on an image in a diffusion process as

$$\frac{\partial I}{\partial t} = \square_2 I ,$$

tend to flatten areas that look alike while enhancing transitions between regions of different characteristics. Such a process showed excellent in identifying anomalies such as man made objects in satellite images mostly compose of natural environment. Refer to Figure 9.

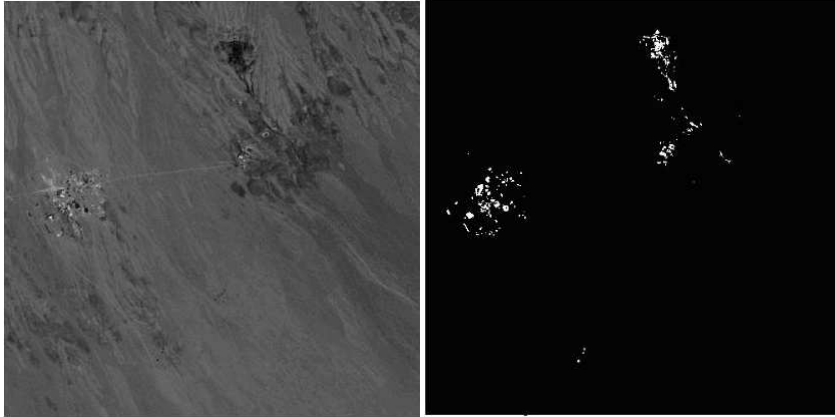


Fig. 9. $\frac{\partial I}{\partial t} = \square_2 I$: On the left the original image is shown while on the right shown the image after diffusion was applied. Notice the enhancement of the man made objects relative to the degradation of the natural environment at the background

Bochner Laplacian for Smoothing In Figure 10 a part of an image is shown, represented as a surface in \mathbb{R}^3 . The part shown in the figure contains some sharp gradient. After 30 iterations of Bochner diffusion

$$\frac{\partial I}{\partial t} = BI = (\square - Curve)I$$

the surface is smoothed apart from the sharp gradient. As such it makes a good candidate for image denoising. In Figure 11 we see a noisy image that is denoised as it goes through diffusion under the Bochner Laplacian.

4 Summary and Future Study

Summary In this paper we introduced diffusion processes that are based on newly developed Laplacian operators for images. The operators are base of a discretized version of the rough and Bochner Laplacian and curvature measures as introduced in [8]. These operators showed good results for a variety of image processing related issues amongst are edge detection sharpening and denoising. Anomaly detection in the context of man-made object detection in satellite imaging was also demonstrated.

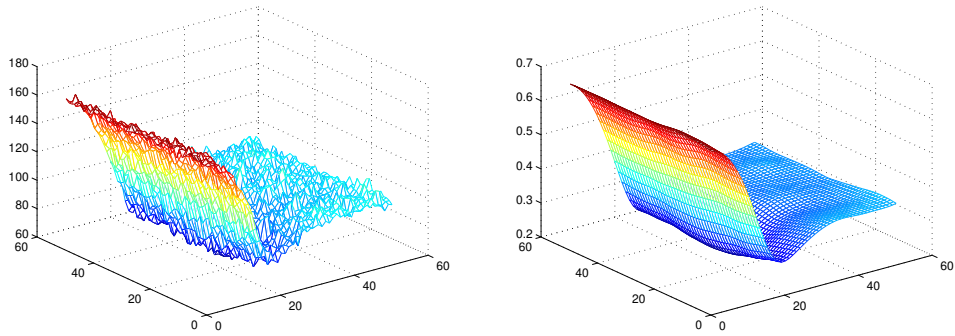


Fig. 10. $\frac{\partial I}{\partial t} = BI = (\square - Curve)I$: On the left, initial surface representation of a gray level image. On the right, the surface smoothed after 30 diffusion iterations using the Bochner Laplacian. The diffused surface is generally smoother than the original alas the sharp gradient (probably an edge in the original image) remains intact.

Current Directions and Future Studies Amongst these we include,

- Implementation of the Laplacians and curvature measures suggested herein to higher dimensions. This is most suitable for computer graphics applications tomography and video processing related issues.
- As the Ricci curvature shows excellent results as an edge detector it used in our current study as a basis for non-linear adaptive interpolation and super-resolution.
- Another application which is in progress is the implementation of the Ricci flow for images. This flow is in fact a diffusion process with the exception that instead of the image, it is its metric that is evolved.

$$\frac{\partial \mathcal{G}(I)}{\partial t} = -2Ric(I) \quad (20)$$

After evolving the metric one has to go through integration phase in order to restore the image out of its gradient field I_x, I_y . In our current study we use the Poisson based technique presented in [2]

References

- [1] Angenent, S., Pichon, E. and Tannenbaum, A., *Mathematical Methods in Medical Image Processing*, Bulletin of AMS, 43, 3, 365-396, 2006.
- [2] Agrawal, A., Raskar, R., and Chellappa, R. *What is the Range of Surface Reconstructions from a Gradient Field?*, ECCV 2006.
- [3] Astola, L. *Multi-Scale Riemann-Finsler Geometry*, PhD Thesis, Eindhoven, 2010.
- [4] Berger, M. *A Panoramic View of Riemannian Geometry*, Springer-Verlag, Berlin, 2003.



Fig. 11. $\frac{\partial I}{\partial t} = BI = (\square - Curve)I$: On the left, Noisy version of Lena while on the right, the image after 10 iterations of diffusion with Bochner Laplacian. The noise significantly reduces yet edges are not affected severely.

- [4] Berger, M. A and Gostiaux B., *Differential Geometry: Manifolds, Curves and Surfaces*, Springer-Verlag, Berlin, 1998.
- [5] Chow, B. and Luo, F. *Combinatorial Ricci Flows on surfaces*, J. Differential Geometry 63, 97-129, 2003.
- [6] Dai J., Luo W., Yau S.-T. and Gu X. *Geometric accuracy analysis for discrete surface approximation*, Geometric Modeling and Processing, 5972, 2006.
- [7] Fuster, A., Astola, L., and Florack, L. *A Riemannian Scalar Measure for Diffusion Tensor Images*, In Proceedings of CAIP 2009, LNCS **5702**, 419426, Springer-Verlag, Berlin, 2009.
- [8] Forman, R. *Bochner's Method for Cell Complexes and Combinatorial Ricci Curvature*, Discrete and Computational Geometry, 29(3), 323-374, 2003.
- [9] Gilboa, G., Sochen, N. and Zeevi, Y. Y. *Forward and Backward Diffusion Processes for Adaptive Image Enhancement and Denoising*, IEEE. Trans. Img. Proc., 2002.
- [10] Glickenstein, D. *A combinatorial Yamabe Flow in three dimensions*, Topology 44, 791-808, 2005.
- [11] Gu, X. and Yau, S. T. *Global Conformal Surface Parameterization*, Proc. Eurographics Symposium on Geometry Processing (2003).
- [12] Jost, J., *Riemannian Geometry and Geometric Analysis*, Springer-Verlag, Berlin, 2002.
- [13] Kimmel, R. Malladi, R. and Sochen, N. *Images as embedded maps and minimal surfaces, movies, color, textures and volumetric medical images*, Int. Jour. Comp. vis., 39, pp.111-129 (2000).
- [14] Leibon, G. and Letscher, D. *Delaunay Triangulations and Voronoi Diagrams for Riemannian Manifolds*, Proceedings of the Sixteenth Annual Symposium on Computational Geometry, 341 - 349, 2000.
- [15] Luo, F., *combinatorial curvature flow for compact 3-manifolds with boundary*, Electronic Research Announcements of the AMS, 11, 12-20, 2005.
- [16] Milnor, J. *Morse Theory* Ann. Math. Stud.
- [17] Morgan, J. and Tian, G. *Ricci flow and the Poincare conjecture*, Clay Mathematics Monographs 3, Providence, R.I., 2007.

- [18] Perlman, G. *The entropy formula for the Ricci flow and its geometric applications*, arxiv:math.DG/0211159, 2002.
- [19] Perlman, G. *Ricci flow with surgery on three-manifolds*, arxiv:math.DG/0303109, 2003.
- [20] Petersen, P. *Riemannian Geometry*, Springer-Verlag, New York, 1998.
- [21] Pizarro, L., Mra'zek, P., Didas, S., Grewenig, S. and Weickert, J. *Generalised nonlocal image smoothing*, Int. Jour. Comp. Vis., to appear.
- [22] Saucan, E., Appleboim, E., and Zeevi, Y. Y. *Sampling and Reconstruction of Surfaces and Higher Dimensional Manifolds*, Journal of Mathematical Imaging and Vision, 30(1), 105-123, 2008.
- [23] Sochen, N. and Zeevi, Y. Y. *Representation of Colored Images by Manifolds Embedded in Higher-Dimensional Non-Euclidean Space* IEEE. Proc. of ICIP98, 1998.
- [24] Sochen, N. *Affine Invariant Flows in the Beltrami Framework*, Jour. of Math. Img. and Vis., 20 133-146, 2004.
- [25] B. M. ter Haar Romeny (ed.), *Geometry-driven diffusion in computer vision*, Kluwer, Dordrecht, 1994.
- [26] Villani, C. *Optimal Transport, Old and New*, Grundlehren der mathematischen Wissenschaften **338**, Springer, Berlin-Heidelberg (2009)
- [27] Weickert, J., *Anisotropic Diffusion in Image Processing*, ECMI Series, Teubner-Verlag, 1998.
- [28] Yakoya, N. and Levine, M. *Range image segmentation based on differential geometry: A hybrid approach*, IEEE Transactions on Pattern Analysis and Machine Intelligence, 11(6), 643-649, 1989.
- [29] Yin, X. Jin, M. Luo, F. and Gu, X. *Discrete Curvature Flow for Hyperbolic 3-manifolds with Complete Geodesic Boundaries*, preprint, 2008.

Acknowledgements Emil Saucan's research supported by the Israel Science Foundation Grant 666/06 and by European Research Council under the European Community's Seventh Framework Programme (FP7/2007-2013) / ERC grant agreement n^o [203134].